

## Determination of Ultrasonic Parameters Based on Attenuation and Dispersion Measurements

PING HE

*Department of Biomedical and Human Factors Engineering  
Wright State University  
Dayton, Ohio 45435  
e-mail: phe@cs.wright.edu*

In the measurement of acoustic attenuation that obeys a power-law  $\alpha = \beta f^n$ , the traditional through-transmission method uses only the amplitude information of the recorded pulses to determine the two parameters,  $\beta$  and  $n$ . In this paper, we propose a new method that utilizes both the amplitude and phase information of the pulses to determine the two parameters. According to this method, the two parameters are estimated by simultaneously performing a least squares fit to the attenuation data that are derived from the amplitude spectra of the pulses, and to the dispersion data that are derived from the phase spectra of the pulses. By fully utilizing the information contained in the recorded pulses and imposing additional constraints on the two parameters, the estimation uncertainty can be reduced. Experimental results from two specimens, one having a linear attenuation and one having a nonlinear attenuation, demonstrate that the new method produces a moderate variance reduction in the case of linear attenuation, and a significant variance reduction in the case of nonlinear attenuation.

KEY WORDS: Attenuation; dispersion; least squares curve fitting; parameter estimation.

### 1. INTRODUCTION

The measurement of acoustic attenuation has important applications in ultrasound tissue characterization and nondestructive material testing.<sup>1-2</sup> For a wide variety of materials, including soft tissues, the attenuation increases with frequency according to a power-law relation:<sup>3,4</sup>

$$\alpha(f) = \beta f^n \quad (1)$$

where  $\beta$  and  $n$  ( $1 \leq n \leq 2$ ) are two material-dependent parameters. Based on such a power-law relation, the measurement of acoustic attenuation reduces to the determination of the two parameters:  $\beta$  and  $n$ .

*In vitro* measurement of acoustic attenuation can be conducted using either a narrowband or broadband through-transmission technique.<sup>4-5</sup> In a typical broadband measurement, two transducers, one for transmitting an ultrasound pulse and one for receiving the pulse, are placed in a water tank. A pulse is first recorded when there is only a water path between the two transducers. The specimen is then inserted in between the two transducers and a second pulse is recorded. From the amplitude spectra of the two pulses, the attenuation is first determined at a number of discrete frequencies, and the two parameters,  $\beta$  and  $n$ , are then estimated by least squares fitting the measured attenuation with a power-law curve. Although this widely used method is quite simple and reasonably accurate in measuring the attenuation, it is often difficult to provide a definite value for each of the two parameters. In some cases, the measured attenuation may be fitted almost equally well with curves associated with different values of  $\beta$  and  $n$ . In other cases, a slight change in the frequency range for curve fitting may result in a significant change in  $\beta$  or/and  $n$ . Ultrasound reflection at the wa-

ter-specimen interface may produce additional uncertainties in determining the individual values of  $\beta$  and  $n$ . In order to effectively reduce the estimation uncertainties, one may have to increase the frequency range for attenuation measurement.

In this paper, we propose a new method for estimating  $\beta$  and  $n$  that can effectively reduce the estimation uncertainties without increasing the frequency range for the measurement. Unlike the traditional method that utilizes only the amplitude information of the two recorded pulses, the new method uses both the amplitude and phase information of the recorded pulses. According to this method, the two parameters,  $\beta$  and  $n$ , are obtained by simultaneously performing a least squares fit to the attenuation data that are derived from the amplitude spectra of the pulses, and to the dispersion data that are derived from the phase spectra of the pulses. By fully utilizing the information contained in the recorded pulses and imposing additional (dispersion) constraints on the two parameters, the estimation uncertainty can be reduced.

The paper is organized as follows. The methods for measuring the attenuation and dispersion using a broadband, through-transmission technique are first reviewed. An emphasis is laid upon a recently developed method for dispersion measurement that is easy to perform and does not require phase unwrapping.<sup>6,7</sup> The models for attenuation and dispersion are then presented. The model for attenuation is based on Eq. (1) and the model for dispersion is based on a time causal model recently proposed by Szabo.<sup>8</sup> After introducing a total squared error (*TSE*) function that is a weighted sum of the difference between the measured and modeled attenuation and the difference between the measured and modeled dispersion, the maximum likelihood estimates for  $\beta$  and  $n$  are derived, first for the case of linear attenuation and then for the case of nonlinear attenuation. Experimental results from two specimens are then reported. The first specimen exhibits a linear attenuation and the second specimen exhibits a nonlinear attenuation. For each specimen, parameters are estimated using both the traditional method and the new method for a number of frequency ranges over which curve fitting is performed. The results show that when the fitting range is gradually decreased, the estimates obtained by the new method are more precise than the estimates obtained by the traditional method. The improvement provided by the new method is more dramatic for nonlinear attenuation.

## 2. METHOD

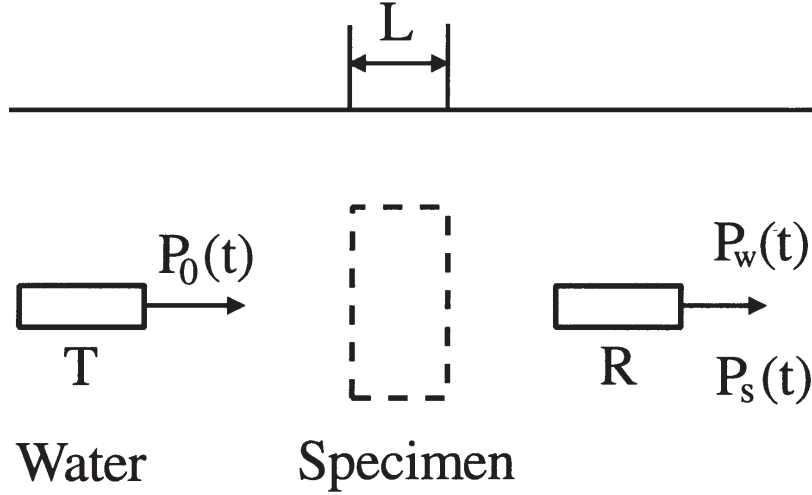
### A. Measurement of attenuation and dispersion

Figure 1 shows the simplified experimental setup for the broadband through-transmission measurement.  $P_w(t)$  represents the received pulse with the water path only, and  $P_s(t)$  represents the received pulse when the specimen is inserted. If we neglect the attenuation of the water, the attenuation of the specimen can be found as:<sup>5</sup>

$$\alpha(f) = \frac{1}{L} \ln T + \frac{1}{L} \ln \left[ \frac{A_w(f)}{A_s(f)} \right] \quad (2)$$

where  $A_w(f)$  and  $A_s(f)$  are the amplitude spectra of  $P_w(t)$  and  $P_s(t)$ , respectively;  $L$  is the thickness of the specimen;  $T = 4z_w z_s / (z_w + z_s)^2$  is the combined transmission coefficient at the two water-specimen interfaces (assuming normal incidence), and  $z_w$  and  $z_s$  are the acoustic impedance of the water and the specimen, respectively.

To measure the dispersion, a method recently proposed by He is used.<sup>6,7</sup> By directly measuring the change in phase velocity between a certain frequency and a reference frequency



**FIG. 1** Experimental set-up for the measurement of attenuation and dispersion using the through-transmission technique.

rather than measuring the absolute phase velocity at any particular frequency, the method eliminates the need for measuring the triggering delays of the sampling window and does not require phase unwrapping which is associated with the annoying  $2m\pi$  phase ambiguity.<sup>9</sup> If we neglect the dispersion of water,<sup>10</sup> the dispersion of the specimen can be found as:<sup>7</sup>

$$v(f) = \frac{1}{V_p(f_0)} - \frac{1}{V_p(f)} = \frac{\phi_w(f) - \phi_s(f)}{2\pi fL} - \frac{\phi_w(f_0) - \phi_s(f_0)}{2\pi f_0L} \quad (3)$$

where  $f_0$  is a reference frequency where the pulses  $P_w(t)$  and  $P_s(t)$  have significant energy;  $V_p$  is the phase velocity;  $\phi_w$  and  $\phi_s$  are the phase spectra of  $P_w(t)$  and  $P_s(t)$ , respectively, after the center of each pulse is circularly shifted to the beginning of the sampling window. In the actual experiment,  $A_w(f)$  and  $A_s(f)$  are obtained by Fast Fourier Transform (FFT). As a result, in the actual calculation, the variable  $f$  in Eqs. (2) and (3) will be replaced by discrete frequencies  $f_i$  ( $i = 1, 2, \dots, N$ ) which cover the entire useful frequency range of  $P_w(t)$  and  $P_s(t)$ .

### B. Traditional method for determining $\beta$ and $n$ — Method 1

The traditional method for determining  $\beta$  and  $n$  is based on attenuation measurement only. Rewrite Eq. (2) in the following form and use discrete frequencies:

$$\bar{u}(f_i) = \frac{1}{L} \ln \left[ \frac{A_w(f_i)}{A_s(f_i)} \right] = \alpha_0 + \alpha(f_i) \quad i = 1, 2, \dots, N \quad (4)$$

where  $\bar{u}(f_i)$  are the measured attenuation data, and  $\alpha_0 = -(\ln T)/L$ . If  $T$  is precisely known, then  $u(f_i)$  are least squares fitted with a curve  $\alpha_0 + \beta f_i^n$ , where  $\beta$  and  $n$  are the only two un-

known parameters. If  $T$  is not precisely known, then  $\alpha_0$  becomes the third unknown parameter in curve fitting. In this study, we consider the more general case of unknown  $T$ .

### C. Proposed method for determining $\beta$ and $n$ — Method 2

Since  $T$  is generally unknown or is difficult to determine accurately, we define a new function  $u(f)$  to eliminate the effects of  $T$ :

$$u(f_i) = \alpha(f_i) - \alpha(f_0) = \frac{\ln A_w(f_i) - \ln A_s(f_i)}{L} - \frac{\ln A_w(f_0) - \ln A_s(f_0)}{L} \quad (5)$$

where  $f_0$  is the same reference frequency in Eq. (3). Comparing Eq. (5) with Eq. (3), one notices the symmetrical way in which the attenuation and dispersion are measured and expressed. As we will show later, this symmetric form of  $u(f)$  and  $v(f)$  helps to determine an optimal weighting factor between the attenuation measurement and dispersion measurements in estimating  $\beta$  and  $n$  by least squares fitting.

According to the power-law relation  $\alpha(f) = \beta f^n$ , the model for  $u(f)$  in Eq. (5) is:

$$u^*(f) = \beta (f^n - f_0^n) \quad (6)$$

To model the dispersion function  $v(f)$  in Eq. (3), we adopt a time causal model developed by Szabo.<sup>8</sup> This model has been found quite accurate for both linear and nonlinear attenuation.<sup>7</sup> Let us first consider the case of linear attenuation ( $n = 1$ ). According to Szabo's model, when  $n = 1$ , the model for dispersion is:

$$v^*(f) = \frac{\beta}{\pi^2} (\ln f - \ln f_0) \quad (7)$$

The same dispersion was also predicted by the nearly local model proposed earlier by O'Donnell et al.<sup>11</sup>

To estimate  $\beta$  based on both the attenuation and dispersion measurements, we define a total squared error ( $TSE$ ) function:

$$TSE = \lambda_1 \sum_{i=1}^N [u(f_i) - u^*(f_i)]^2 + \lambda_2 \sum_{i=1}^N [v(f_i) - v^*(f_i)]^2 \quad (8)$$

where  $u(f)$ ,  $u^*(f)$ ,  $v(f)$ ,  $v^*(f)$  are defined in Eqs. (5), (6), (3) and (7), respectively. The two parameters,  $\lambda_1$  and  $\lambda_2$ , in Eq. (8) have two roles. First of all, they are needed due to the fact that  $u(f)$  and  $v(f)$  have different units. Secondly, they are introduced to derive an optimal weighting factor between the attenuation and dispersion measurements in estimating the value of  $\beta$ . Substituting the models for attenuation ( $u^*$ ) and dispersion ( $v^*$ ) as defined in Eqs. (6) and (7), and solving for  $\beta$  based on the equation:  $\frac{\partial(TSE)}{\partial\beta} = 0$ , we obtain the optimal (maximum

likelihood) estimate of  $\beta$  that minimizes the  $TSE$ :

$$\beta = \frac{k \sum_{i=1}^N u_i (f_i - f_0) + \frac{1}{\pi^2} \sum_{i=1}^N v_i (\ln f_i - \ln f_0)}{k \sum_{i=1}^N (f_i - f_0)^2 + \frac{1}{\pi^4} \sum_{i=1}^N (\ln f_i - \ln f_0)^2} \quad (9)$$

where  $k = \lambda_1 / \lambda_2$  is a new parameter,  $u_i = u(f_i)$ , and  $v_i = v(f_i)$ . Now let us find the optimal value of  $k$  that minimizes the variance of the  $\beta$  estimate. If we use  $\sigma_u^2$  and  $\sigma_v^2$  to represent the mean variance of the attenuation measurement and dispersion measurement, respectively, the variance of the  $\beta$  estimate can be obtained as:<sup>12</sup>

$$\begin{aligned} \sigma_{\beta}^2 &= \sum_{i=1}^N \left[ \left( \frac{\partial \beta}{\partial u_i} \right)^2 \sigma_{u_i}^2 + \left( \frac{\partial \beta}{\partial v_i} \right)^2 \sigma_{v_i}^2 \right] \\ &= \frac{k^2 \sigma_u^2 \sum_{i=1}^N (f_i - f_0)^2 + \frac{1}{\pi^4} \sigma_v^2 \sum_{i=1}^N (\ln f_i - \ln f_0)^2}{\left[ k \sum_{i=1}^N (f_i - f_0)^2 + \frac{1}{\pi^4} \sum_{i=1}^N (\ln f_i - \ln f_0)^2 \right]^2} \end{aligned} \quad (10)$$

where  $\sigma_{u_i}^2$  and  $\sigma_{v_i}^2$  are the variance of each measurement  $u_i$  and  $v_i$ , respectively. In deriving Eq. (10), we assume  $\sigma_{u_i}^2 = \sigma_u^2$  and  $\sigma_{v_i}^2 = \sigma_v^2$ . By solving  $\frac{\partial(\sigma_{\beta}^2)}{\partial k} = 0$ , we obtain the optimal value of  $k$  that minimizes  $\sigma_{\beta}^2$ :

$$k = \frac{\lambda_1}{\lambda_2} = \frac{\sigma_v^2}{\sigma_u^2} \quad (11)$$

Since the actual values of  $\sigma_u^2$  and  $\sigma_v^2$  are unknown, we further assume that  $\sigma_u^2$  and  $\sigma_v^2$  are proportional to the mean square values of the measured attenuation and dispersion, respectively:

$$k = \frac{\lambda_1}{\lambda_2} = \frac{\sigma_v^2}{\sigma_u^2} \cong \frac{\sum_{i=1}^N v_i^2}{\sum_{i=1}^N u_i^2} \quad (12)$$

By substituting this value of  $k$  into Eq. (9), we obtain the optimal estimate of  $\beta$  based on the measured attenuation and dispersion:

$$\beta = \frac{\sum_{i=1}^N v_i^2 \sum_{i=1}^N u_i (f_i - f_0) + \frac{1}{\pi^2} \sum_{i=1}^N u_i^2 \sum_{i=1}^N v_i (\ln f_i - \ln f_0)}{\sum_{i=1}^N v_i^2 \sum_{i=1}^N (f_i - f_0)^2 + \frac{1}{\pi^4} \sum_{i=1}^N u_i^2 \sum_{i=1}^N (\ln f_i - \ln f_0)^2} \quad (13)$$

In addition, by using Eq. (12), we may redefine the total squared error as:

$$TSE = \frac{\sum_{i=1}^N [u_i - \beta (f_i - f_0)]^2}{\sum_{i=1}^N u_i^2} + \frac{\sum_{i=1}^N \left[ v_i - \frac{\beta}{\pi^2} (\ln f_i - \ln f_0) \right]^2}{\sum_{i=1}^N v_i^2} \quad (14)$$

For nonlinear attenuation ( $n > 1$ ), Szabo's time causal model gives the following expression of dispersion:<sup>8</sup>

$$v^*(f) = -\frac{\beta \tan(n\pi/2)}{2\pi} (f^{n-1} - f_0^{n-1}) \quad (15)$$

A new total squared error function, similar to the one in Eq. (14) can then be defined based on the nonlinear attenuation and nonlinear dispersion models:

$$TSE = \frac{\sum_{i=1}^N [u_i - \beta (f_i^n - f_0^n)]^2}{\sum_{i=1}^N u_i^2} + \frac{\sum_{i=1}^N \left[ v_i + \frac{\beta \tan(n\pi/2)}{2\pi} (f_i^{n-1} - f_0^{n-1}) \right]^2}{\sum_{i=1}^N v_i^2} \quad (16)$$

In this case, there are no closed-form solutions for  $\beta$  and  $n$ . To find the optimal estimates of these two parameters that minimize  $TSE$ , one may perform an iterative grid search with two parameters  $\beta$  and  $n$ .<sup>13</sup> On the other hand, the speed of the search can be significantly increased if we perform a one-parameter search. To do this, we first show that for any given  $n$ , the optimal value of  $\beta$  that minimizes  $TSE$  in Eq. (16) has a closed-form solution:

$$\beta = \frac{\sum_{i=1}^N v_i^2 \sum_{i=1}^N u_i (f_i^n - f_0^n) - \frac{\tan(n\pi/2)}{2\pi} \sum_{i=1}^N u_i^2 \sum_{i=1}^N v_i (f_i^{n-1} - f_0^{n-1})}{\sum_{i=1}^N v_i^2 \sum_{i=1}^N (f_i^n - f_0^n)^2 + \frac{\tan^2(n\pi/2)}{4\pi^2} \sum_{i=1}^N u_i^2 \sum_{i=1}^N (f_i^{n-1} - f_0^{n-1})^2} \quad (17)$$

The one-parameter search routine contains the following steps: (i) specify an initial value for  $n$  and an increment step  $\Delta n$ ; (ii) find  $\beta$  using Eq. (17); (iii) calculate  $TSE$  in Eq. (16) using the current values of  $\beta$  and  $n$ ; (iv) increment  $n$  by  $\Delta n$ , calculate the new values of  $\beta$  and  $TSE$ ; (v) compare the new value of  $TSE$  with the previous value of  $TSE$ , if decreased, go back to step (iv); if increased, let  $\Delta n = -\Delta n$ ; and then go back to step (iv). This process continues until  $TSE$  no longer changes. The final values of  $\beta$  and  $n$  are the optimal estimates.

### 3. EXPERIMENT AND RESULTS

To test the new method, a through-transmission experiment is conducted using two specimens: a cylindrical block made of Plexiglas that exhibits a linear attenuation, and a phantom made of castor oil that exhibits a nonlinear attenuation. The Plexiglas block has a diameter of 6.3 cm and a thickness ( $L$ ) of 4 cm. To make the castor oil phantom, the two ends of a plastic tube (inner diameter = 7.6 cm,  $L = 5.5$  cm) are sealed with thin polyethylene film, and the tube is then filled with castor oil. The transmitting and receiving transducers used in this study are Panametrics V382 (3.5MHz, 13 mm aperture, 8.9 cm focal distance) and V384 (3.5MHz, 6.35 mm aperture, nonfocusing), respectively. The distance between the two transducers is 18 cm, and the water temperature is 22°C. A Panametrics 5052PR pulse/receiver is used to drive the transmitting transducer and receives the transmitted pulse. The output from the receiver is digitized by a Sony/Tek 390AD programmable digitizer that has a 10-bit resolution and a sampling frequency of 60 MHz. Each sampling window contains

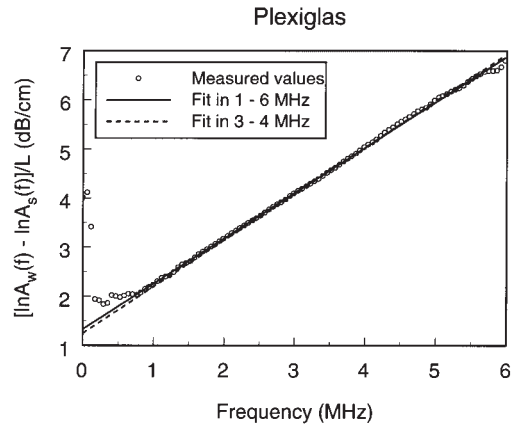


**FIG. 2** Parameter estimation using the traditional method for the Plexiglas specimen. The circles represent the measured attenuation. The solid line ( $1.328 + 0.925f$ ) is the fitted least squares line in the frequency range of 1-6 MHz, and the dashed line ( $1.245 + 0.947f$ ) is the fitted least squares line in the range of 3-4 MHz.

1,024 samples and the sampled pulses are averaged 20 times to improve the signal-to-noise ratio.

For the Plexiglas specimen, the useful frequency range for measuring the attenuation and dispersion is found to be from 1 MHz to 6 MHz. The reference frequency ( $f_0$ ) is chosen as the central frequency 3.5 MHz. The attenuation and dispersion are calculated according to Eqs. (4), (5) and (3), respectively. The measured attenuation exhibits a linear frequency dependence. The parameter  $\beta$  is first estimated using Method 1 (the traditional method) by fitting the measured attenuation,  $u(f_i)$ , with a straight line  $\alpha_0 + \beta f$ , where  $\alpha_0$  is also an unknown parameter. To test the variability of the  $\beta$  estimate, curve fitting is performed in four additional frequency ranges: 1.5-5.5 MHz, 2-5 MHz, 2.5-4.5 MHz, and 3-4 MHz. The mean and standard deviation of the five  $\beta$  estimates are then calculated. For Method 2 (the proposed method), the parameter  $\beta$  is calculated using Eq. (13). Again, five values of  $\beta$  are obtained for the above five frequency ranges, and the mean and standard deviation are then calculated.

For the castor oil phantom, the useful frequency range is found to be from 1 MHz to 5 MHz, and a reference frequency  $f_0 = 3$  MHz is chosen. The measured attenuation of this specimen shows a marked nonlinear frequency dependence. As a result, nonlinear curve fitting is employed. For Method 1, the values of  $\beta$  and  $n$  are estimated by fitting the measured attenuation,  $u(f_i)$ , with a power curve  $\alpha_0 + \beta f^n$  where  $\alpha_0$ ,  $f$  and  $n$  are three unknown parameters. For Method 2, the values of  $\beta$  and  $n$  are estimated using the one-parameter search routine that includes Eq. (17), as described earlier. For each method, parameter estimation is performed in four different frequency ranges: 1-5 MHz, 1.5-4.5 MHz, 2-4 MHz, and 2.5-3.5 MHz, and the mean and standard deviation of the  $\beta$  and  $n$  estimates are again calculated.

Figure 2 shows the  $\beta$  estimation made on the Plexiglas specimen using the traditional method that performs curve fitting using the attenuation data only. For this specimen,  $n = 1$  and only  $\beta$  needs to be estimated. The circles represent the measured attenuation,  $u(f_i)$ , using Eq. (4). The solid line is obtained by performing least squares fitting in the frequency range of 1-6 MHz. The dashed line is obtained by performing least squares fitting in the frequency range of 3-4 MHz. Figure 3 shows the  $\beta$  estimation using the new method that simultaneously performs curve fitting on the attenuation data (Fig. 3a) and the dispersion data (Fig. 3b). Again, the solid lines are obtained for the fitting range of 1-6 MHz and the dashed lines are obtained for the fitting range of 3-4 MHz. By comparing figure 2 with figure 3(a), one notices that the solid line and the dashed line in figure 3(a) are closer to each other than the two lines in figure 2, indicating that the variability of  $\beta$  estimation using the new method

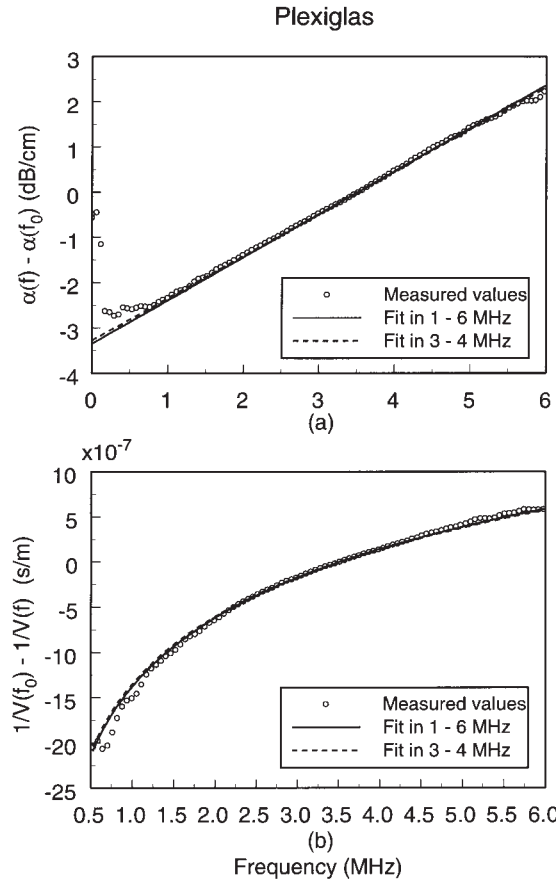


**FIG. 3** (a) Parameter estimation using the new method for the plexiglas specimen. The circles represent the measured differential attenuation. The reference frequency  $f_0$  is 3.5 MHz. The solid line [ $0.954(f-f_0)$ ] is the simultaneously fitted (together with the curve in figure 3(b)) least squares line in the frequency range of 1-6 MHz, and the dashed line [ $0.933(f-f_0)$ ] is the simultaneously fitted least squares line in the range of 3-4 MHz. (b) The circles represent the measured dispersion. The reference frequency  $f_0$  is 3.5 MHz. The solid line [ $0.0967(\ln f - \ln f_0)$ ] is the simultaneously fitted (together with the curve in figure 3a) least squares line in the frequency range of 1-6 MHz, and the dashed line [ $0.0945(\ln f - \ln f_0)$ ] is the fitted least squares line in the range of 3-4 MHz.

**TABLE 1**

Comparison of two methods in estimating  $\beta$  of the Plexiglas specimen. The unit of  $\beta$  is  $\text{dB}\cdot\text{cm}^{-1}\cdot\text{MHz}^{-1}$ .

Fitting range (MHz)	Method 1 $\beta$	Method 2 $\beta$
1.0 - 6.0	0.925	0.956
1.5 - 5.5	0.935	0.955
2.0 - 5.0	0.944	0.951
2.5 - 4.5	0.955	0.946
3.0 - 4.0	0.947	0.933
mean	0.941	0.948
standard deviation	0.012	0.009

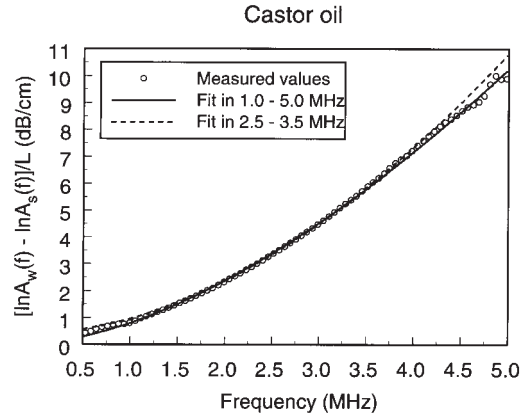


**FIG. 4** Parameter estimation using the traditional method for the castor oil specimen. The circles represent the measured attenuation. The solid line ( $0.038 + 0.764f^{0.61}$ ) is the fitted least squares line in the frequency range of 1-5 MHz, and the dashed line ( $0.419 + 0.545f^{1.833}$ ) is the simultaneously fitted least squares line in the range of 2.5-3.5 MHz.

**Table 2**

Comparison of two methods in estimating  $\beta$  and  $n$  of the castor oil specimen. The unit of  $\beta$  is  $\text{dB}\cdot\text{cm}^{-1}\cdot\text{MHz}^{-n}$ .

Fitting range (MHz)	Method 1		Method 2	
	$\beta$	$n$	$\beta$	$n$
1.0 - 5.0	0.764	1.611	0.702	1.666
1.5 - 4.5	0.716	1.661	0.704	1.674
2.0 - 4.0	0.642	1.732	0.696	1.687
2.5 - 3.5	0.545	1.833	0.686	1.697
mean	0.667	1.709	0.697	1.681
s.d.	0.095	0.096	0.008	0.014

is smaller. The detailed results of  $\beta$  estimation using the two methods are listed in table 1. Method 1 refers to the traditional method and Method 2 refers to the proposed method. The table lists the  $\beta$  estimate obtained in each of the five fitting ranges using each method. The means of  $\beta$  estimates using the two methods are almost the same (0.941 vs. 0.948), but the standard deviation of  $\beta$  estimates using the new method (0.009) is 25% smaller than that of the traditional method (0.012).

Figures 4 and 5 show the parameter estimation performed on the castor oil phantom, and table 2 lists the  $\beta$  and  $n$  estimates obtained in each of the four fitting ranges using the two methods. Again, by comparing figure 4 with figure 5(a), one notices that the solid curve (with fitting range of 1-5 MHz) and the dashed curve (with fitting range of 2.5-3.5 MHz) in figure 5(a) are much closer to each other than the two curves in figure 4. According to table 2, the standard deviation of  $\beta$  estimate using Method 2 is 12 times smaller than that of Method 1, and the standard deviation of  $n$  estimate is 7 times smaller.

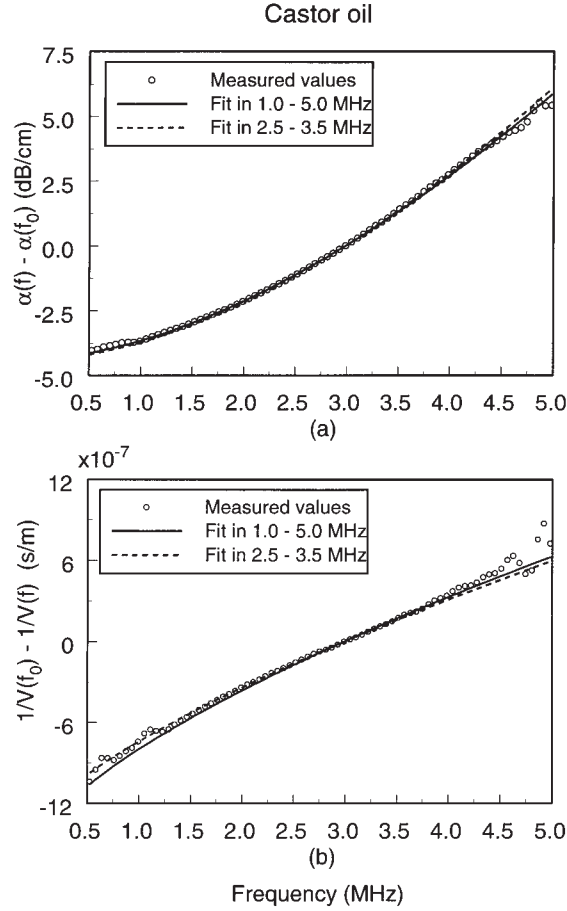


**FIG. 5** (a) Parameter estimation using the new method for the castor oil specimen. The circles represent the measured differential attenuation. The reference frequency  $f_0$  is 3 MHz. The solid line [ $0.702 (f^{0.666} - f_0^{1.666})$ ] is the simultaneously fitted (together with the curve in figure 5b) least squares line in the frequency range of 1-5 MHz, and the dashed line [ $0.686 (f^{0.697} - f_0^{1.697})$ ] is the simultaneously fitted least squares line in the range of 2.5-3.5 MHz. (b) The circles represent the measured dispersion. The reference frequency  $f_0$  is 3.5 MHz. The solid line [ $0.065 (f^{0.666} - f_0^{0.666})$ ] is the simultaneously fitted (together with the curve in figure 5a) least squares line in the frequency range of 1-5 MHz that corresponds to  $\beta = 0.702$  and  $n = 1.666$ , and the dashed line [ $0.056 (f^{0.697} - f_0^{0.697})$ ] is the simultaneously fitted least squares line in the range of 2.5-3.5 MHz that corresponds to  $\beta = 0.686$  and  $n = 1.697$ .

#### 4. CONCLUSION AND DISCUSSION

A new method is proposed for estimating the two acoustic parameters,  $\beta$  and  $n$ , that uses both the amplitude and phase information of the recorded pulses in a through-transmission measurement. This new method is built upon two recent developments involving acoustic dispersion: (a) A time causal model was developed by Szabo<sup>8</sup> that provides explicit and accurate relations between the dispersion and the two parameter  $\beta$  and  $n$ , as defined by Eqs. (7) and (15). Together with Eq. (1), these three equations indicate that  $\beta$  and  $n$  should be considered as two fundamental material parameters rather than just two attenuation parameters. Consequently, determination of these two parameters based on both attenuation and dispersion measurement is a more logical approach. (b) A method was proposed by He<sup>6,7</sup> that makes the measurement of dispersion (from the phase spectra of the recorded pulses in a through-transmission experiment) as easy as the measurement of attenuation (from the am-

plitude spectra). Because the phase information is readily available in a through-transmission experiment, the improvement in parameter estimation is achieved without additional cost.

The main advantage of the proposed method is achieving a variance reduction in estimating  $\beta$  and  $n$ . The major premise is that the phase spectra of the transmitted pulse provide additional information, independent of that of the amplitude spectra, about the true values of  $\beta$  and  $n$ . Based on this premise, we now give a more quantitative analysis on the variance reduction in estimating  $\beta$  for the case of linear attenuation. The variance of the  $\beta$  estimate using the traditional method based on Eq. (4) can be formulated as:<sup>12</sup>

$$\sigma_{\beta}^2 = \frac{N\sigma^2}{N \sum_{i=1}^N f_i^2 - \left( \sum_{i=1}^N f_i \right)^2} \tag{18}$$

where  $N$  is the number of *independent* sample points and  $\sigma^2$  is the variance of each sample  $u(f_i)$ . Expand  $f_i$  around a center frequency  $f_0$  so that  $f_i = f_0 + i \Delta f$ , for  $i = 0, \pm 1, \pm 2, \dots, \pm k$ , where  $2k + 1 = N$ , and use the relations:  $\sum i = 0$ , and  $\sum i^2 = N(N^2 - 1)/12 \cong N^3/12$ , we obtain

$$\sigma_{\beta}^2 \cong \frac{12\sigma^2}{NB^2} \tag{19}$$

where  $B = N\Delta f$  is the frequency range used for curve fitting. Equation (19) indicates that the variance of the  $\beta$  estimate can be reduced by increasing  $N$  or/and  $B$ . A caution about the number  $N$  is in order. For a particular pair of recorded pulses  $P_u(t)$  and  $P_s(t)$ , the effective value of  $N$ , or the maximum number of *independent* sample points  $u(f_i)$ , is fixed. Although the actual number of sample points used for curve fitting can be arbitrarily increased by first padding zeros to the recorded pulses and then performing FFT, such a process only adds correlated samples but will not increase the effective value of  $N$ . Since the added zeros do not contain any information about  $\beta$ , the process of zero padding should not reduce  $\sigma_{\beta}^2$ . On the other hand, the phase spectra of the pulses contain additional information about  $\beta$ . By simultaneously fitting an attenuation curve and a dispersion curve, the dispersion samples (which has the same number as the attenuation samples) impose additional constraints to the  $\beta$  estimate. As a result, the effective value of  $N$  is increased. Based on this analysis, if the dispersion curve is also a straight line (actually it is not), the new method would decrease  $\sigma_{\beta}^2$  approximately by a factor of 2. From table 1,  $\sigma_{\beta}^2$  of the new method is 1.78 times smaller than that of the traditional method, indicating the actual variance reduction in this particular experiment is less than, but close to 2 times. For the nonlinear attenuation, the quantitative analysis of variance reduction is rather difficult. From table 2,  $\sigma_{\beta}^2$  of the new method is 141 times smaller, and  $\sigma_n^2$  is 47 times smaller than that of the traditional method, respectively. These results indicate that the variance reduction in the case of nonlinear attenuation is much more dramatic.

From tables 1 and 2, one may also notice that  $\sigma_{\beta}^2$  of the traditional method for the case of nonlinear attenuation is significant larger (63 times) than  $\sigma_{\beta}^2$  of the same method for the case of linear attenuation. An obvious reason is that in nonlinear attenuation curve fitting, there are three unknown parameters,  $\beta$ ,  $n$  and  $\alpha_0$ , while in linear attenuation curve fitting, there are only two unknown parameters,  $\beta$  and  $\alpha_0$ . Some researchers have tried to fix the parameter  $\alpha_0$  by calculating the value of the transmission coefficient  $T$  in Eq. (4) based on the measurement of the material properties.<sup>5</sup> There are two problems with this approach. Firstly, it is sometime very difficult to determine the exact value of  $T$ . For example, the castor oil phantom used in this study has a thin polyethylene film that separates the castor oil from the water.

For such a water-specimen interface,  $T$  will be very difficult to determine due to the presence of this film. Secondly, if there is an error in determining  $T$ , this error will produce significant bias, or systematic error, in  $\beta$  and  $n$  estimation. The method proposed in this study achieves significant variance reduction without such a risk.

It should be pointed out that the discussion so far about the variance reduction is based on a random error model for attenuation and dispersion measurements. In the actual measurement, there are many sources that produce systematic errors. For example, if the frequency response of the receiver is not perfectly flat within the frequency range of interest, the estimated  $\beta$  and  $n$  will be biased. Systematic errors can also be produced by the diffraction effects<sup>14,15</sup> and nonlinear propagation effects.<sup>16,17</sup> There is no general method to analyze and remove systematic errors. However, the proposed method may still have some advantages over the traditional method even in the presence of systematic errors. This statement is based on the fact that the amplitude spectra and the phase spectra of the transmitted pulses are in general affected by the various error sources in different ways. In some cases, the bias of the estimate may be unnoticeable when only the attenuation curve is fitted, but may be revealed by the large residual errors when both the attenuation curve and the dispersion curve are fitted simultaneously. In other cases, the effects of the error sources on the amplitude spectra and phase spectra may be partially canceled each other so that the final bias of the estimated parameter is reduced. To verify these advantages however, more rigorous analysis and careful experiments are needed.

## REFERENCES

1. Bamber, J.C., Hill, C.R., Acoustic properties of normal and cancerous human liver – I: Dependence on pathological condition, *Ultrasound Med. Biol.* 7, 121-133 (1981).
2. Kline, R.A., Measurement of attenuation and dispersion using an ultrasonic spectroscopy technique, *J. Acoust. Soc. Am.* 76, 498-504 (1984).
3. Hill, C. R. Ultrasonic attenuation and scattering by tissues, in *Handbook of Clinical Ultrasound* (M. de Vieger et al, eds.), pp. 91-98 (Wiley, New York, 1978).
4. Narayana, P.A., Ophir, J., On the validity of the linear approximation in the parametric measurement of attenuation in tissues, *Ultrasound Med. Biol.* 9, 357-361 (1983).
5. Lee, C.C., Lahham, M., and Martin, B.G., Experimental verification of the Kramers- Kronig relationship for acoustic waves, *IEEE Trans. Ultrason. Ferroelec. Freq. Contr.* 37, 286-294 (1990).
6. He, P., On the measurement of ultrasonic dispersion using a broadband pulse technique (abstract), *Ultrasonic Imaging* 20, 74, (1998).
7. He, P., Direct measurement of ultrasonic dispersion using a broadband transmission technique *Ultrasonics* 37, 67-70 (1999).
8. Szabo, T.L., Causal theories and data for acoustic attenuation obeying a frequency power law, *J. Acoust. Soc. Am.* 97, 14-24 (1995).
9. Mobley, J., Marsh, J.N., Hall, C.S., Hughes, M.S., Brandenburger G.H., and Miller, J. G., Broadband measurements of phase velocity in Albunex<sup>®</sup> suspensions, *J. Acoust. Soc. Am.* 104, 2145 – 2153 (1998).
10. Rokhlin, S.I., Lewis, D.K., Graff, K.F., and Adler, L., Real-time study of frequency dependence of attenuation and velocity of ultrasonic waves during the curing reaction of epoxy resin, *J. Acoust. Soc. Am.* 79, 1786-1793 (1986).
11. O'Donnell, M., Jaynes, E.T., and Miller, J.G., Kramers-Kronig relationship between ultrasonic attenuation and phase velocity, *J. Acoust. Soc. Am.* 69, 696-701 (1981).
12. Bevington, P.R., Least-squares fit to a straight line, in *Data Reduction and Error Analysis for the Physical Sciences*, pp. 92-118 (McGraw-Hill, New York, 1969).
13. Bevington, P. R., Least-squares fit to an arbitrary function, in *Data Reduction and Error Analysis for the Physical Sciences*, pp. 204-246 (McGraw-Hill, New York, 1969).

14. Xu, W., and Kaufman, J.J., Diffraction correction methods for insertion ultrasound attenuation estimation, *IEEE Trans. Biomed. Eng.* 40, 563-569 (1993).
15. Kaufman, J.J., and Xu, W., Diffraction effects in insertion mode estimation of ultrasonic group velocity, *IEEE Trans. Ultrason. Ferroelect. Freq. Contr.* 42, 232-242 (1995).
16. Zeqiri, B., Errors in attenuation measurements due to nonlinear propagation effects, *J. Acoust. Soc. Am.* 91, 255- 2593 (1991).
17. Wu, J., Effects of nonlinear interaction on measurements of frequency-dependent attenuation coefficients, *J. Acoust. Soc. Am.* 99, 3380 - 3384 (1996).